

# Biosorption potential of neem leave powder for the sequestration of arsenic and chromium metal ions

Anandh Babu M.<sup>1</sup>, Hemavathi S.<sup>2</sup>, Kousalyadevi G.<sup>3\*</sup> and Shanmuga Priya S.P.<sup>4</sup>

<sup>1</sup>Department of Civil Engineering, PSN College of Engineering and Technology, Tirunelveli-627152, Tamilnadu, India

<sup>2</sup>Department of Civil Engineering, K Ramakrishnan College of Technology, Trichy-621112, Tamilnadu, India

<sup>3</sup>School of Architecture and Interior Design, SRM Institute of Science and Technology, kattankulathur campus-603203, Tamilnadu, India

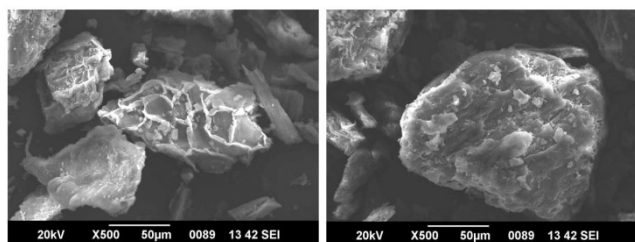
<sup>4</sup>Department of Chemical Engineering, Mohamed Sathak Engineering College, Kilakarai-623517, Tamilnadu, India

Received: 07/08/2023, Accepted: 14/09/2023, Available online: 20/09/2023

\*to whom all correspondence should be addressed: e-mail: kousym.arch@gmail.com

<https://doi.org/10.30955/gnj.005287>

## Graphical abstract



## Abstract

In this study, neem leaf biosorbent, prepared through chemical synthesis and activated with concentrated sulfuric acid, was utilized as an organic adsorbent for the removal of heavy metal ions, specifically arsenic (As) and chromium (Cr), from wastewater. The characteristics of the biosorbent were thoroughly analyzed using BET, FTIR, SEM, and EDX analysis to evaluate the surface morphology and functional groups. The experimental results indicated that under optimal conditions, with a pH of 10.0, a biosorbent dose of 3 g/L, an initial concentration of 20 mg/L, and a contact time of 60 minutes, 89.74% of As (II) and 82.32% of Cr(VI) metal ions were efficiently removed from synthetic solutions. To understand the nature of the adsorption process, various isothermal studies were conducted to determine whether it was homogeneous or heterogeneous. In addition to the above-mentioned experiments, kinetic studies were conducted to assess the physical or chemical nature of the metal ion adsorption on the adsorbent. Thermodynamic investigations were also performed to determine whether the adsorption of metal ions was exothermic or endothermic and whether the process was spontaneous. The results from the desorption studies revealed that the addition of 0.3N HCl resulted in the highest rate of desorption. This effectively facilitated the recovery of the metal ions from the spent adsorbent, indicating the effectiveness of 0.3N HCl in desorbing the adsorbed metal ions.

**Keywords:** Biosorption, neem laves, heavy metals, batch studies, desorption studies

## 1. Introduction

Water holds an indispensable position in the environment, serving a crucial purpose in supporting life on Earth. It takes on different states - liquid, solid (ice), and gas (water vapor) - and undergoes a perpetual journey through the hydrosphere, atmosphere, lithosphere, and biosphere, commonly referred to as the water cycle or hydrological cycle. Water's importance within the environment encompasses several facets. Firstly, it is essential for the survival and development of all living beings, constituting the primary building block of cells for plants, animals, and humans alike. Secondly, water significantly contributes to sustaining biodiversity in aquatic ecosystems, such as rivers, lakes, oceans, and wetlands, by offering habitats, nourishment, and breeding sites for countless species. Access to clean and safe drinking water is imperative for human well-being, yet regrettably, numerous regions continue to face the challenge of unreliable water sources, resulting in health concerns. Furthermore, water assumes a critical role in numerous industrial processes and energy generation, including its utilization in cooling systems for power plants. Sustainable water management is of utmost importance to avert depletion and pollution, safeguarding this precious resource for the future (Priya *et al*, 2022). Recognizing the significance of water in the environment and embracing sustainable practices to utilize and conserve it are essential for upholding a healthy and harmonious ecosystem. Although the planet possesses an abundance of water, numerous regions experience water scarcity due to factors such as population growth, excessive consumption, pollution, and the effects of climate change. Such scarcity can often escalate into conflicts over water resources. Human activities, including industrial discharges, agricultural runoff, and improper waste disposal, frequently lead to water pollution,

rendering water bodies unfit for drinking and adversely impacting aquatic ecosystems and biodiversity. This poses a threat to low-lying coastal areas and islands, leading to habitat loss and potential displacement of populations. These events can have devastating effects on communities, agriculture, and ecosystems (Batagarawa *et al.*, 2019). Pollution and habitat destruction in aquatic environments can lead to the decline and extinction of species that rely on these ecosystems for survival.

To tackle these challenges effectively, it is vital to embrace sustainable water management practices, advocate water conservation, invest in clean technologies, and enforce policies that safeguard water resources and guarantee equitable access to clean water for everyone. Furthermore, global cooperation is indispensable in addressing transboundary water issues and working towards a more sustainable and resilient water future. Water pollution refers to the contamination of water bodies, including lakes, rivers, oceans, groundwater, and aquifers, with harmful substances, making them unsuitable for various purposes. Human activities, such as industrial discharges, agricultural runoff, and domestic sewage, are the main culprits behind water pollution (Sirusbakht *et al.*, 2018). Additionally, natural factors can also contribute to this problem. Industrial discharges are responsible for releasing toxic chemicals, heavy metals, and organic compounds into water bodies. The excessive use of fertilizers, pesticides, and herbicides in agriculture results in agricultural runoff, causing eutrophication and posing a threat to aquatic life. Moreover, improperly treated domestic sewage contains pathogens and chemicals that further contribute to water pollution and the degradation of water sources. Oil spills from ships and oil rigs can cause severe devastation to marine environments, disrupting ecosystems and harming marine life. Mining operations release heavy metals and toxic substances into water bodies, further contributing to water pollution and ecosystem degradation. Landfills generate leachate, a liquid that seeps out and contaminates groundwater and nearby water sources, posing a significant environmental hazard (Venkatraman *et al.*, 2021). Moreover, pollutants present in the air dissolve in rainwater, leading to acid rain and contributing to water pollution.

Water pollution has dire consequences, affecting various aspects of life. It poses significant health risks to humans by causing waterborne diseases, which can be severe and even fatal. Moreover, water pollution disrupts aquatic ecosystems, leading to adverse impacts on biodiversity and fisheries, affecting the delicate balance of underwater life. To address the issue of water pollution, a range of measures must be taken (Adeyemo *et al.*, 2015). These encompass effective treatment of wastewater, the promotion of sustainable agricultural practices, strict enforcement of regulations concerning industrial discharges, and the implementation of response plans for oil spills. Additionally, the use of green infrastructure can aid in decreasing stormwater runoff and filtering out pollutants. Moreover, raising public awareness and

encouraging water conservation efforts are crucial aspects in tackling this environmental challenge. In this research, Neem Powder was employed as a means to eliminate heavy metal ions, specifically Arsenic and Chromium, from wastewater. Neem Powder has been the subject of investigation due to its potential in effectively removing heavy metals from water. Neem, scientifically known as *Azadirachta indica*, is a tree native to the Indian subcontinent, and its seeds and leaves are recognized for their medicinal and pesticidal attributes. The presence of specific compounds in neem, such as tannins, saponins, and alkaloids, could potentially facilitate its capacity to adsorb heavy metals from water.

## 2. Materials and methods

### 2.1. Stock and biochar preparation

The preparation of the stock solution involved adding 100 mg of  $As_4O_6$  &  $K_2Cr_2O_7$  powder separately to 1 liter of distilled water. This resulted in a concentration of 100 mg/L for each substance in the stock solution. For the batch studies, the concentrations were adjusted as needed based on the specific experimental requirements. To prepare the adsorbent, neem leaves were collected and thoroughly washed multiple times to remove any dust and impurities. The washed neem leaves were then dried under sunlight for about 10 hours. Next, the dried neem leaves were subjected to further treatment in a muffle furnace at a temperature of 200°C for 24 hours. Neem leaves were intended to be transformed into biochar, an activated adsorbent substance, using this technique. After being removed from the muffle furnace, the biochar adsorbent was cleaned with double-distilled water to get rid of any remaining impurities and other contaminants. Following this, the washed adsorbent material was transferred to an oven and heated at 80°C for additional drying before being utilized for batch experimental studies. This drying process ensured that the adsorbent was completely free from moisture, making it suitable for further experiments. This process ensured the preparation of a clean and activated adsorbent material from neem leaves for the subsequent adsorption experiments on Arsenious Oxide and Potassium dichromate solutions.

### 2.2. Pore distribution & BET surface area

Pore Distribution and BET Surface Area are crucial measurements used to characterize the porous nature of materials, especially adsorbents like activated carbon or zeolites, which find extensive use in various applications. Pores are small empty spaces or voids within the material's structure that provide sites for adsorption of molecules. The pore distribution is determined through techniques like nitrogen adsorption isotherms (Kołodzyńska *et al.*, 2016). The adsorption isotherms provide data on the amount of nitrogen gas adsorbed at different relative pressures. This data is then used to calculate the pore size distribution using models such as the Barrett-Joyner-Halenda (BJH) method or the Density Functional Theory (DFT). On the other hand, the BET surface area is a critical measurement that quantifies the total surface area available for adsorption per unit mass of

the material. It is determined by the BET theory, which is based on the adsorption of nitrogen gas molecules on the material's surface (Bouras *et al*, 2015). The BET equation is expressed in equation 1:

$$\frac{C_a}{C_m} = \frac{P}{P_0} \times \frac{1}{(C_m - 1)} + \frac{C_a}{C_m} \quad (1)$$

Where:  $C_a$  = Amount of nitrogen gas adsorbed at a given relative pressure (P).

$C_m$  = Monolayer capacity of the adsorbent.

P = Pressure of the nitrogen gas.

$P_0$  = Saturation pressure of nitrogen gas.

To determine the BET surface area, a plot of  $\frac{C_a}{C_m}$  against  $\frac{P}{P_0}$  is generated, and linear regression analysis is applied to the data. The slope and intercept of the line yield the values for  $C_m$  and  $C_a$ , respectively, which allow for the calculation of the BET surface area. In summary, the pore distribution and BET surface area are essential measurements in understanding the adsorption capacity and accessibility of porous materials. These measurements play a crucial role in material selection and design for applications such as gas separation, water purification, catalysis, and the removal of pollutants from air or water. Materials with a well-controlled pore distribution and high BET surface area are preferred due to their superior adsorption capabilities and efficiency.

### 2.3. Batch adsorption studies

Batch adsorption studies are experimental investigations aimed at evaluating the adsorption performance of neem leaf powder as an adsorbent for the removal of heavy metals, such as arsenic and chromium, from contaminated solutions. Neem leaf powder, known for its porous structure and active compounds, has the potential to efficiently adsorb these toxic heavy metals from water sources. In the batch adsorption experiment, a known quantity of neem leaf powder is added to a measured volume of the heavy metal-contaminated solution. The mixture is thoroughly mixed or stirred to ensure uniform contact between the neem leaf powder and the heavy metal ions. The mixture is then left to equilibrate under controlled conditions, such as constant temperature and agitation, for a specific time to reach adsorption equilibrium. The adsorption capacity (q) of neem leaf powder for arsenic and chromium can be evaluated using equation 2.

$$q_t = \frac{(C_o - C_e) V}{m} \quad (2)$$

Where:

$q_t$  = Adsorption capacity of neem leaf powder (mg/g)

$C_o$  &  $C_e$  = Initial & Final concentration of metal ions in the solution (mg/L)

V = Volume of the contaminated solution (L)

m = Mass of neem leaf powder used (g)

After equilibration, samples of the contaminated solution are collected, and the final concentrations of arsenic and

chromium (Ce) are measured using atomic adsorption spectroscopy. The data obtained from the batch adsorption studies can also be used to construct adsorption isotherms to understand the adsorption behavior of neem leaf powder for these heavy metals. The results obtained from batch adsorption studies provide valuable information on the adsorption efficiency of neem leaf powder for arsenic and chromium removal. This data can guide the optimization of process conditions, such as the adsorbent dosage, contact time, and initial concentrations of heavy metals, to enhance the adsorption performance. Neem leaf powder's adsorption capabilities make it a promising and eco-friendly option for water treatment and environmental remediation to tackle heavy metal contamination and safeguard public health and the environment.

### 2.4. Isotherm study

The adsorption isotherm helps to reveal the nature of adsorption, whether it follows a monolayer or multilayer process, and provides insights into the adsorption capacity and affinity of the adsorbent for the specific adsorbate. The following types of isotherm studies were conducted in this batch adsorption process.

#### 2.5. Langmuir isotherm

The Langmuir isotherm model is applied to the experimental data to determine the adsorption capacities and constants for each metal at different temperatures (Hong *et al*, 2020). Equation 3 contains the Langmuir isotherm equation for metal ion adsorption.

$$\frac{C_e}{q_e} = \frac{1}{q_m} + \frac{C_e}{K_L} \quad (3)$$

where:

$C_e$  = Metal ion concentration in the solution at equilibrium (mg/L)

$q_e$  = metal ion adsorbed amount at equilibrium (mg/g)

$q_m$  = Neem leaf powder's maximum monolayer adsorption capability (mg/g)

$K_L$  = Adsorption energy-related Langmuir constant (L/mg)

#### 2.6. Freundlich isotherm

Furthermore, this isotherm model is applied to derive the Freundlich constants and exponents for both metals at different temperatures. The Freundlich isotherm for metal ion adsorption is expressed in equation 4.

$$\ln q_e = \ln k_f + \frac{1}{n} \ln C_e \quad (4)$$

where:

$C_e$  = Metal ion concentration in the solution at equilibrium (mg/L)

$q_e$  = metal ion adsorbed amount at equilibrium (mg/g)

$K_f$  = Freundlich constant related to adsorption capacity (mg/g)

n = Freundlich exponent related to adsorption intensity

By analyzing the isotherm data and calculating the relevant parameters, this study provides valuable insights

into the adsorption behavior of neem leaf powder for arsenic and chromium removal under different temperature conditions. These findings facilitate the optimization of heavy metal removal processes and showcase neem leaf powder's potential as an eco-friendly and effective adsorbent for water treatment and environmental remediation applications.

### 2.7. Temkin isotherm

The Temkin isotherm study investigates the adsorption behavior of neem leaf powder for arsenic and chromium removal from contaminated solutions. The Temkin isotherm is given by the equation 5.

$$q_{eq} = \frac{RT}{b} \ln K_T + \frac{RT}{b} \ln C_e \quad (5)$$

It is used to simulate the adsorption process, with  $q_{eq}$  representing the amount of arsenic or chromium adsorbed at equilibrium (mg/g),  $R$  representing the gas constant (8.314 J/(molK)),  $T$  representing the absolute temperature in Kelvin (K),  $b$  representing the Temkin constant related to heat of adsorption (J/mol), and  $C_e$  representing the equilibrium binding constant (L/g). Experimental data is collected by exposing neem leaf powder to solutions with varying initial concentrations of arsenic and chromium at different temperatures. After achieving adsorption equilibrium, the final concentrations of arsenic and chromium in the solutions are measured. By plotting  $q_e$  against  $\ln(C_e)$  and performing linear regression, the Temkin constants ( $b$ ) and equilibrium binding constants ( $C_e$ ) are determined for each metal at different temperatures.

The Temkin isotherm study provides valuable insights into the adsorption mechanism, considering the non-uniform distribution of heat of adsorption. It helps in understanding the interactions between neem leaf powder and heavy metals, guiding the optimization of removal processes for efficient arsenic and chromium removal (Revellame *et al.*, 2020). The results contribute to the potential application of neem leaf powder as an eco-friendly adsorbent in water treatment and environmental remediation to combat heavy metal pollution and ensure water resource protection.

### 2.8. D-R isotherm

In the Dubinin-Radushkevich (D-R) isotherm study, the adsorption behavior of neem leaf powder for arsenic and chromium removal from contaminated solutions is investigated. The D-R isotherm model is commonly used for microporous materials and is based on the assumption of a Gaussian distribution of adsorption energies (Singh *et al.*, 2018). The equation for the D-R isotherm is given by (Eqn. 6):

$$\ln q_e = \ln x_m - \beta \epsilon^2 \quad (6)$$

$q_e$  – Equilibrium time metal ion adsorption

$x_m$  – Adsorption capacity

The D-R isotherm study provides valuable insights into the adsorption mechanism of neem leaf powder for arsenic and chromium removal, especially in microporous

environments. The calculated Dubinin-Radushkevich monolayer adsorption capacity ( $q_e$ ) and the constant ( $\beta$ ) offer information about the adsorption energetics and the suitability of neem leaf powder as an adsorbent for these heavy metals. The temperature effect analysis guides the design of effective adsorption systems and optimizes the removal efficiency. This study demonstrates the potential application of neem leaf powder as an environmentally friendly and efficient adsorbent for water treatment and environmental remediation, effectively addressing arsenic and chromium contamination and ensuring the preservation of water resources.

### 2.9. Kinetic studies

Kinetic studies are essential to understand the rate of adsorption of arsenic and chromium onto neem leaf powder. The following kinetic studies were adopted in this batch adsorption study to evaluate the adsorption performance using neem leaf biochar.

#### 2.10. Pseudo-first order kinetic model

The Pseudo-First Order kinetic model implies that the rate of adsorption is linearly proportional to the difference between the initial concentration ( $q_e$ ) and the concentration at any given time ( $t$ ). The linear mathematical representation of this kinetic model was represented in Equation 7.

$$\log(q_e - q) = \log q_e - \frac{k}{2.303} t \quad (7)$$

where:

$q_e$  = Metal ion concentration at time  $t$  (mg/L)

$q$  = Initial concentration of metal ions (mg/L)

$K$  = Pseudo-First Order rate constant (1/s)

#### 2.11. Pseudo-second order kinetic model

The pseudo-second-order model is based on the idea that chemisorption, which involves the sharing or exchange of electrons between the adsorbent surface and the adsorbate molecules, is the rate-limiting stage in the adsorption process. This model is particularly applicable to adsorption processes where chemisorption is the dominant mechanism (Konicki *et al.*, 2017). By fitting experimental data to this model, one can gain insights into the adsorption rate and the mechanisms involved in the adsorption process, which are crucial for understanding and optimizing adsorption processes in various applications, including water treatment and wastewater remediation. The Pseudo-Second Order kinetic model posits that the rate of adsorption is proportional to the square of the difference between the initial concentration ( $q$ ) and the concentration at any given time ( $q_e$ ). The equation for the Pseudo-Second Order kinetic model is given by Eqn. 8:

$$\frac{t}{q} = \frac{1}{h} + \frac{1}{q_e} t \quad (8)$$

where:

$q$  = Amount of metal ions adsorbed at time  $t$  (mg/g)

$q_e$  = Amount of metal ions adsorbed at equilibrium (mg/g)

$h$  = Pseudo-Second Order rate constant (g/(mg·min))

### 2.12. Boyd kinetic model

The Boyd kinetic model, also known as the intraparticle diffusion model, investigates the adsorption process's rate-limiting stage. This model helps to identify whether the adsorption is controlled by intraparticle diffusion, suggesting that the transport of adsorbate molecules within the adsorbent pores is the rate-controlling step (Aydina *et al*, 2021). The Boyd kinetic model is a power function model that accounts for both film diffusion and intraparticle diffusion processes. The Boyd kinetic model is represented in equation 9.

$$Bt = -0.4977 - \ln(1 - F) \quad (9)$$

The experimental data and its linearity were assessed using the  $B_t$  vs.  $t$  plot and the coefficient of diffusion ' $D_i$  ( $m^2/s$ )' was calculated using Equation 10.

$$B = \frac{\Pi^2 D_i}{r^2} \quad (10)$$

The effective diffusion coefficient ( $D_i$ ) provides information about how fast the adsorbate diffuses within the adsorbent material and into its internal pores or active sites. A higher  $D_i$  value indicates faster diffusion, which is generally favorable for efficient adsorption. The radius of the adsorbent particles ( $r$ ) can be determined from sieve analysis, which is a common method used to measure the particle size distribution of the adsorbent material. By calculating the radius, one can gain insights into the pore structure and surface area of the adsorbent, which are crucial factors influencing its adsorption capacity. Both ' $D_i$  and  $r$ ' are valuable parameters in adsorption studies, as they provide essential information about the transport of adsorbates within the adsorbent material and the characteristics of the adsorbent itself, helping to optimize the adsorption process and design effective water treatment strategies. These kinetic studies provide valuable insights into the adsorption rate and mechanisms of neem leaf powder for arsenic and chromium removal (Phuengphai *et al*, 2021). The determined rate constants and equilibrium adsorption capacity help in understanding the adsorption kinetics and guide the selection of appropriate contact times for efficient heavy metal removal using neem leaf powder as an adsorbent.

## 3. Results and discussion

### 3.1. Adsorbent's characterization

In batch adsorption investigations, the properties of the neem leaf biosorbent material play a crucial role. To confirm its ability to remove targeted pollutants, a characterization study was conducted. This study involved various analyses to test the properties and functional groups of the material, including the following investigations: FTIR, SEM, EDX & BET surface analysis. These analyses provided valuable insights into the structure and composition of the biosorbent material, helping to understand its potential as an effective adsorbent for pollutant removal.

### 3.2. FTIR studies

The FTIR images shown in Figure 1 (a) and (b) revealed the occurrence of numerous efficient groups in the organized neem leaf biochar before and after taking up of Arsenic and Chromium metal ions respectively. The energy band ranging from  $2860\text{ cm}^{-1}$  to  $3420\text{ cm}^{-1}$  exhibited a very high peak, indicating the presence of  $-\text{CH}_2$  and  $-\text{OH}$  groups. Furthermore, within the bandwidth of  $1000\text{ cm}^{-1}$  to  $1800\text{ cm}^{-1}$ , several functional elements were observed: water at  $1620\text{ cm}^{-1}$ , ambiances of aromatic complexes among  $1400\text{ cm}^{-1}$  and  $1600\text{ cm}^{-1}$ , bending vibrations of  $-\text{CH}_2$  groups at  $1350\text{ cm}^{-1}$ , and C-O vibration stretching at  $1000\text{ cm}^{-1}$ . Additionally, at the  $1000\text{ cm}^{-1}$  level, aromatic ring vibrations were observed, and lower frequencies showed the stretching of  $-\text{OH}$  ions (Fideles, *et al*, 2019). These observations demonstrate that the prepared biochar adsorbent contains a significant amount of active functional groups capable of adsorbing pollutants from various sources.

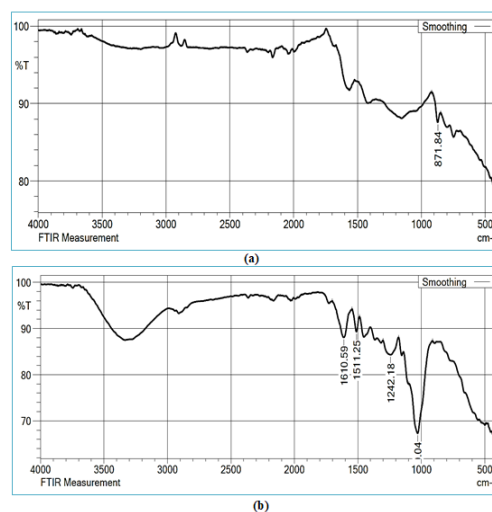


Figure 1. FTIR spectra for biochar adsorbent (a) before and (b) after chemical activation

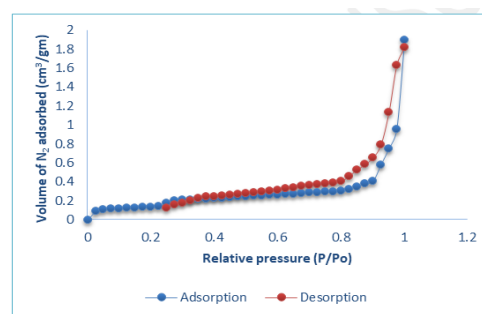


Figure 2. Surface area analysis of neem leaf biosorbent

### 3.3. Pore and surface area distribution analysis

The neem leaf biochar's surface area and size of pores could be calculated by evaluating the nitrogen adsorption and desorption isotherm curve at  $-196^\circ\text{C}$ , as illustrated in Figure 2. There are both micro and meso holes in the adsorbent, according to the type II isotherm that the adsorption process followed (Labied *et al*, 2018). The existence of micropores is shown by the first curve on the isotherm, while the presence of mesopores is represented by the second curve in the sawdust adsorbent. The

activated neem leaf biosorbent's meso and micropore diameters are shown in Table 1, and its surface area is

**Table 1.** Size and pore characteristics of neem leaf biosorbent

Sl. No.	Adsorbent Property	Measured Unit	Measured value
1.	Adsorbent's Surface Area (BJH analysis)	$\text{m}^2 \text{g}^{-1}$	78.483
2.	Adsorbent's pore volume	$\text{cc g}^{-1}$	0.212
3.	Adsorbent's Pore Radius	$\text{\AA}$	44.373
4.	Adsorbent's Surface Area (BET analysis)	$\text{m}^2 \text{g}^{-1}$	3.12
5.	Adsorbent's pore diameter – Average value	nm	0.061

### 3.4. Microscopic analysis

The surface of raw and metal ions adsorbed neem leaf biochar was shown in Figure 3 (a) & (b) respectively. Before the addition of the metal ion-containing solution, the adsorbent's surface (Figure 3a) displayed numerous active sites, which are crucial for adsorbing contaminants from the aqueous medium. Upon allowing the neem leaf biosorbent to interact with the metal ion-containing solution until saturation occurred, the SEM picture in Figure 3b illustrates the surface of the activated neem leaf biosorbent after absorbing As and Cr metal ions. Once the saturation point was reached, all of the active sites became filled with contaminants, leaving no vacant spaces on the surface. The visual proof of the adsorption process was demonstrated by the accumulation of pollutants on the uppermost of the biosorbent surface, forming a cloud-like structure.

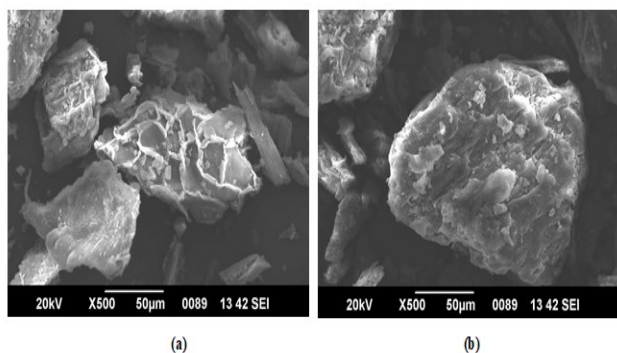


**Figure 3.** Scanning Electron Microscope analysis of neem leaf biochar (a) Raw & (b) Metal ions loaded respectively

### 3.5. X-ray analysis

To assess the metal ion adsorption on the surface of the adsorbent, EDX analysis was utilized. Figure 4(a) presents the EDX image of the neem leaf adsorbent before the absorption of metal ions from the aqueous solutions. In this image, numerous organic and inorganic components were observed, including carbon, oxygen, and calcium. Figure 4(b) shows the peak distribution picture of the neem leaf adsorbent after being exposed to metal ion solutions. The presence of the necessary metal ions can be seen in this image, suggesting that the adsorption process is efficient (Wang *et al.*, 2022). Additionally, the EDX analysis revealed the presence of other organic and inorganic elements, such as calcium, silicon, and iron. This comprehensive analysis provides valuable information about the composition of the adsorbent surface and confirms the successful adsorption of metal ions.

smaller than that of other commercial activated carbons at  $3.12 \text{ m}^2/\text{g}$ .

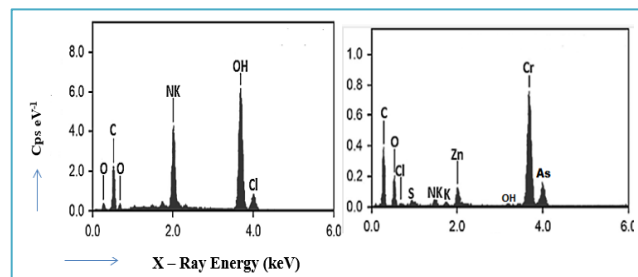


**Figure 4.** EDX plots of biosorbent material, (a) before and (b) after taking the pollutants

## 4. Batch adsorption experiments

### 4.1. Impact of pH

The effect of pH on the adsorption of metal ions was investigated in the synthetic solution with pH values ranging from 2.0 to 12.0. During the experiment, the contact time was set to 60 minutes, and the dose of neem leaf biosorbent used was  $1 \text{ g/L}$ . The concentration of each metal ion in the solution was kept constant at  $20 \text{ mg/L}$  throughout the study. This standardized setup allowed for a consistent and controlled examination of the metal ion adsorption process. The study aimed to understand how changes in pH influence the adsorption behavior. Figure 5 illustrates the correlation between the adsorbent's capacity to absorb metal ions and the pH of the solution. It is evident from the graph that the adsorption capacity increases with the rising pH of the solution. This indicates that the adsorbent's efficiency in removing metal ions improves as the pH of the solution increases. This can be attributed to the presence of charged adsorbent sites with a positive nature, which interact with the neem leaf biosorbent. At higher pH levels, the adsorbent surface becomes more positively charged, leading to a more efficient removal of metal ions from the solution (Dulla *et al.*, 2020). The results suggest that the pH of the solution plays a significant role in enhancing the adsorption process, particularly at higher pH values where the positive charge on the adsorbent surface promotes rapid metal ion elimination. This information is crucial in optimizing the adsorption process and designing effective water treatment strategies using neem leaf biosorbent.

As depicted in Figure 5, the adsorbent exhibited the highest quantity of metal ion absorption at a pH of 10.0. However, beyond this pH, the metal ion elimination gradually decreased. This finding suggests that the optimal pH for maximum metal ion removal by the adsorbent is around 10.0, and deviations from this pH level can result in reduced adsorption efficiency. This



decrease in adsorption efficiency can be attributed to the precipitation of metal hydroxides at higher pH values, leading to reduced availability of metal ions for adsorption. At the optimum pH of 10.0, the neem leaf activated carbon demonstrated remarkable adsorption capacities, removing 87.12% of As ions and 92.28% of Cr ions from the solution. This confirms the excellent adsorption performance of the neem leaf activated carbon for these specific metal ions under the given conditions. The findings highlight the importance of pH control in the adsorption process to achieve optimal removal of metal ions (Benjelloun *et al*, 2021). Indeed, based on the experimental data, neem leaf activated carbon demonstrates efficient adsorption properties for removing As and Cr ions from polluted water sources.

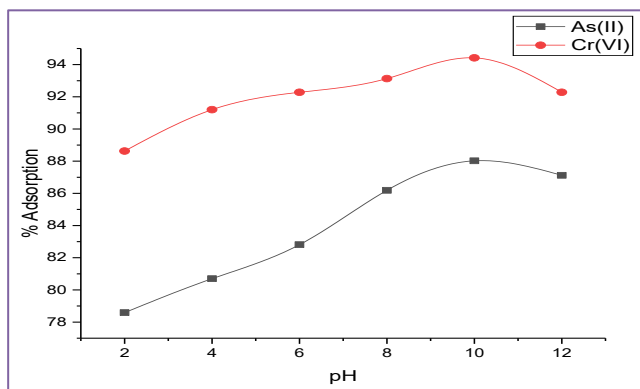


**Figure 5.** Changes in adsorption efficiency by altering solution's pH

#### 4.2. Impact of neem leaf dose

The amount of neem leaf biochar present has a substantial impact on the amount of pollutants that may be adsorbed in the synthetic solution, as illustrated in Figure 6. While retaining the solution's pH at 10.0, the metal ion concentration 20 mg/L, and the contact time at 60 minutes, the dose level of the adsorbent was adjusted in the batch mode of the experiment. According to the data, the dosage of neem leaf biochar increased along with the metal ion absorption. biochar had the maximum adsorption effectiveness for heavy metal removal. The adsorbent displayed a strong capacity to remove metal ions from the solution at this dose level, resulting in a significant improvement in adsorption efficiency. Furthermore, it was observed that at this optimal dosage of 3 g/L, the concentration gradient had minimal impact on the removal of metal ions from the solution. This finding indicates that the adsorbent's active sites were efficiently utilized and saturated, leading to a plateau in the removal efficiency. Thus, 3 g/L can be considered the optimal dose to achieve maximal adsorption efficiency in the context of the experimental conditions tested. These findings emphasize the significance of selecting an appropriate dosage level of neem leaf biochar to optimize the removal of pollutants from contaminated water sources (Regti1 *et al*, 2017). A dosage level of 3 g/L was found to be the most effective in this study, providing valuable insights for the practical application of neem leaf biochar as an adsorbent in water treatment processes.

The increase in metal ion uptake with an increase in biochar dose is attributed to the availability of more free active surface area to adsorb the molecules. In this study, the neem leaf biochar dose of 3 g/L was found to be particularly effective, resulting in the adsorption of 80.48% of As and 70.28% of Cr metal ions from the aqueous solutions. This indicates that increasing the dosage of neem leaf biochar enhances its adsorption capacity, leading to higher pollutant removal efficiency (Xi *et al*, 2020). The optimal dosage of 3 g/L offers a good balance between surface area availability and pollutant adsorption, making it a favorable choice for efficient water purification applications.

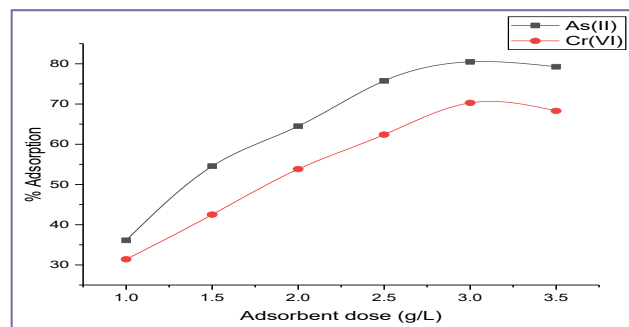


**Figure 6.** Changes in adsorption efficiency by varying neem leaf biochar dose

#### 4.3. Impact of contact time

The adsorption process is influenced by the contact time between the pollutants and the adsorbent material. This study altered the contact time from 10 to 80 minutes while varying the As and Cr ions concentration in the aqueous solutions from 20 to 100 mg/L. The pH of the solution was held constant at 10.0 throughout the trial, while the biochar dosage remained constant at 3 g/L. The availability of active and unoccupied sites in the adsorbent material caused the initial quantity of metal ion uptake to occur quickly, as shown in Figure 7(a) and (b). The process did, however, achieve a saturation threshold for the metal ion adsorption into the mesopores of the biochar (Hosseinzehi *et al*, 2020). This suggests that the adsorbent's active sites were efficiently utilized, and further increases in the metal ion concentration or contact time did not significantly enhance the adsorption capacity beyond a certain point. The figure demonstrates that the maximum efficiency was achieved within 60 minutes of contact time, indicating that this duration is sufficient to achieve optimal pollutant removal. Beyond 60 minutes, there was no significant improvement in adsorption efficiency, suggesting that prolonged contact time may not yield further benefits in terms of pollutant uptake. Adsorption efficiency is the measure of how well metal ions are absorbed by the adsorbent at a constant rate as the adsorption process moves forward. Adsorption efficiency is influenced by things like surface repulsion, mass transfer restrictions, and energy barriers for pore penetration (Haro *et al*, 2021). The maximum efficiency of 86.34% for As and 89.83% for Cr metal ions was observed in this study with an optimum contact time of 60 minutes and metal ion concentration of 20 mg/L.

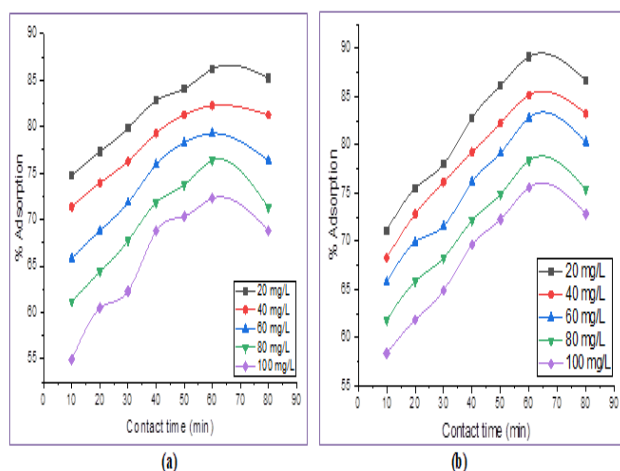


**Figure 7.** Changes in adsorption efficiency by altering Contact time for (a) As & (b) Cr metal ions

#### 4.4. Impact of ion concentration

The investigation highlights that high metal ion concentrations in aqueous solutions pose environmental risks and can impact the adsorption effectiveness of activated adsorbent materials. In this study, the concentration of each metal ion was varied from 20 to 100 mg/L to understand its influence on the adsorption efficiency. The experimental conditions included a groundnut shell charcoal dose of 3 g/L, a solution pH of 10.0, and a contact time of 60 minutes. As illustrated in Figure 8, metal ion adsorption occurred rapidly at lower concentrations, indicating that the adsorbent effectively removed metal ions from the solution. However, as the ion concentration in the aqueous solutions steadily increased, the rate of targeted ions and its absorption decreased. This observation indicates that at higher concentrations, the adsorbent's active sites may become saturated or inhibited, leading to a reduced capacity for metal ion removal. Hence, optimizing the metal ion concentration is essential to achieve maximum adsorption efficiency in water treatment processes (Malti *et al.*, 2022). At low metal ion concentrations, the adsorption process was rapid due to the abundance of large active sites on the adsorbent surface. As the metal ions were absorbed, the adsorbent reached its saturation point in the mesopores (Stefanik *et al.*, 2018). In this batch study, a concentrated metal ion solution of 20 mg/L showed high adsorption efficiency using neem leaf biosorbent. At low concentrations, the activated adsorbent material demonstrated remarkable adsorption capabilities, effectively removing up to 98.63% of As and 87.29% of Cr metal ions from the solution. The rapid uptake of metal ions at these lower concentrations indicates that the adsorbent has not yet reached its saturation point, and there are still vacant active sites available for further adsorption. This suggests that the adsorbent's capacity is not yet fully utilized, and it can continue to adsorb more metal ions from the solution at these concentrations. It also indicates the potential of the adsorbent to efficiently treat water contaminated with low concentrations of metal ions.

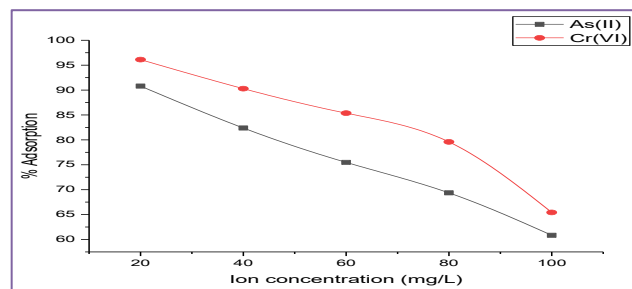


**Figure 8.** Adsorption efficiency modifications caused by changing metal ion concentrations

#### 4.5. Impact of temperature

The results at various temperatures show that temperature has a major impact on the adsorption of metallic ions using neem leaf biosorbent. The highest reduction in metallic ions was observed at 20°C, and as the temperature increased, the efficacy of metallic ion removal gradually decreased, as illustrated in Figure 9a for As and Figure 9b for Cr heavy metals, respectively. The adsorption activity on the neem leaf biochar's surface was reduced with an increase in temperature, leading to decreased efficiency. Furthermore, the reduction in metal ion removal as temperature increases shows that the adsorption process is exothermic, generating heat (Manjuladevi *et al.*, 2018). Based on this observation, it can be inferred that the adsorption of metal ions onto neem leaf powder involves an exothermic process. The decrease in surface activity at higher temperatures may be attributed to factors such as desorption or alterations in the surface chemistry of the adsorbent. These findings highlight the importance of considering temperature as a critical parameter in optimizing the adsorption process using neem leaf biosorbent for the removal of metallic ions from water sources. From this study, 93.83% of As and 89.47% of Cr metal ions removal was observed at an optimum temperature of 20°C.

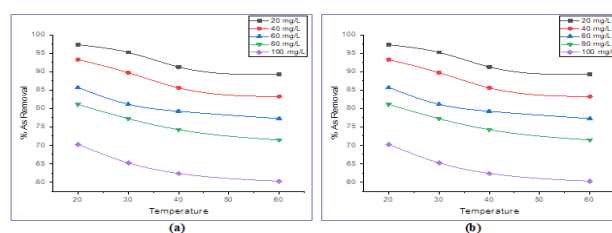


**Figure 9.** Changes in adsorption efficiency by varying solution's temperature for (a) As & (b) Cr metal ions

### 5. Isotherm studies

#### 5.1. Langmuir study

Langmuir isotherm experimentations were carried out to assess the removal of metal ions onto the adsorbent, hence characterising metal transport between the solid and liquid phases. The Langmuir isotherm model is often used to analyse physical-force-driven monolayer adsorption processes (Agarwal *et al.*, 2016). In this study, the uniform adsorption of metal ions was evaluated by plotting  $C_e/q_e$  against  $C_e$ , as shown in Figure 10 for chromium and lead heavy metal ions. However, the obtained regression values ( $R^2$ ) for each plot were less



than 0.95, suggesting that the Langmuir isotherm model was not applicable to describe the adsorption behavior in this specific case. The isotherm model constants obtained from the experimental data were presented in Table 2. However, these values did not align with the adsorption process. To further evaluate the metal ion adsorption, the separation factor, also known as the equilibrium parameter or dimensionless constant ( $R_L$ ), was utilized. The efficacy of the adsorption process by the adsorbent is shown by the crucial parameter known as the  $R_L$  value, which has a range of 0 to 1. According to the  $R_L$  values in this experimental work, the adsorption of metal ions by the neem leaf adsorbent did not adhere to a monolayer process with a physical mode of heterogeneous activity. Positive adsorption circumstances are indicated by  $R_L$  values less than 1, while negative adsorption conditions are indicated by  $R_L$  values larger than 1. In some circumstances,  $R_L$  values equal to 1 indicate that the adsorption process is occurring at the favourable threshold.

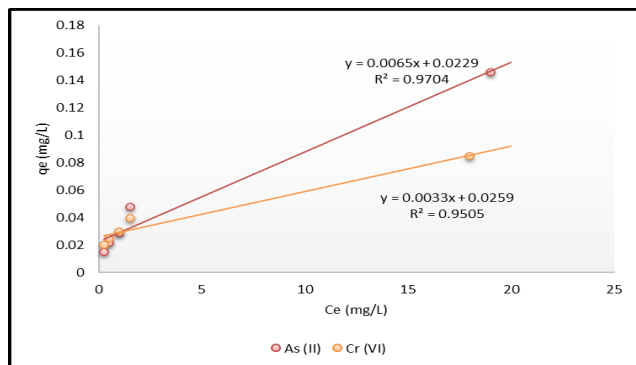


**Figure 10.** Langmuir isotherm plot for the adsorption of heavy metals using neem leaf biochar

### 5.2. Freundlich study

Freundlich isotherm studies were conducted to investigate the multilayer adsorption process by chemical mode. Linear plots of  $\ln C_e$  against  $\ln q_e$  were used to analyze the adsorption of arsenic and chromium heavy metal ions, as shown in Figure 11. The regression values ( $R^2$ ) obtained from these plots were high ( $>0.95$ ), demonstrating that Freundlich isotherm investigations are appropriate for analyzing metal ion adsorption. The Freundlich isotherm model constants were assessed and are reported in Table 2. The good connection between the predicted and calculated constant values implies that the Freundlich isotherm model matches the metal ion adsorption process effectively. This confirms that the adsorption of metal ions by the neem leaf adsorbent follows a chemical mode and dynamic multilayer adsorption. Moreover, the adsorption process exhibited a heterogeneous nature during the uptake of pollutants by the biosorbent (Omer *et al.*, 2022). The successful application of the Freundlich isotherm model and the agreement between expected and calculated values further support the effectiveness of the neem leaf adsorbent for removing metal ions from aqueous solutions. Understanding the adsorption behavior and mode is essential for optimizing the use of this adsorbent in water treatment applications.

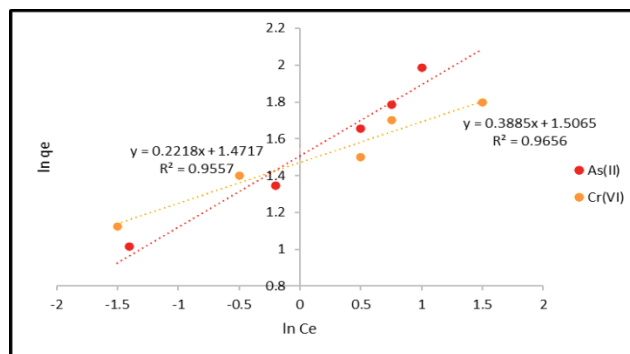


**Figure 11.** Freundlich isotherm plot for the adsorption of heavy metals using neem leaf biochar

### 5.3. Temkin isotherm study

The bio-adsorbent demonstrated a remarkable capability for adsorbing metal ions from aqueous solutions. Various parameters, including pore size, pore volume, and specific surface area, were determined through adsorption isotherm studies to describe the adsorbent material. The adsorption process of heavy metal ions (As and Cr) by neem leaf biochar was further investigated using the Temkin isotherm model to gain insights into the adsorbent's characteristics. Figure 12 depicts the Temkin plots ( $q_e$  vs.  $C_e$ ) and from these plots, the kinetic constants ( $K_T$  and  $b$ ) were calculated. The Temkin isotherm model was found to be a good fit for the adsorption process at a temperature of 30°C, as indicated by the high  $R^2$  values presented in Table 2. This fitting process with the Temkin isotherm model allows for the evaluation of binding energies and the uniform distribution of adsorption sites. Furthermore, the significant amount of metal ion adsorption indicates that a monolayer adsorption process occurs during the contacts between the adsorbent and the metal ions (Condurache *et al.*, 2022). This finding highlights the efficiency of neem leaf biochar as an adsorbent material for removing heavy metal ions from water sources, making it a promising candidate for water treatment applications.

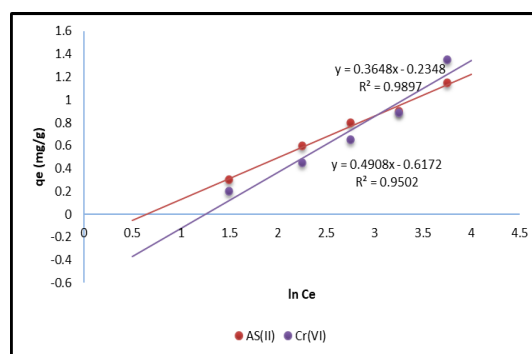


**Figure 12.** Temkin isotherm plot for heavy metal adsorption using biochar made from neem leaves

### 5.4. D-R isotherm study

The Dubinin-Radushkevich (D-R) isotherm model is a valuable tool for investigating the adsorption process and characterizing the adsorbent material's composition. In this study, the D-R isotherm was working to analyze the metal ions (arsenic and chromium) and its adsorption by neem leaf biochar at 30°C. Figure 13 displays the plots of

the D-R isotherm, where  $\ln q_e$  (the natural logarithm of the adsorption capacity) is plotted against  $\epsilon^2$  (the Polanyi potential). This type of plot helps to assess the feasibility of the D-R isotherm model for describing the adsorption process. Table 2 lists the relevant constants obtained from the D-R isotherm model. These constants are important for characterizing the pollutant removal and understanding the adsorption behavior of the metal ions on the neem leaf biochar. The regression coefficient ( $R^2$ ) values are used to evaluate how well the experimental data fit the D-R isotherm model.  $R^2$  values greater than 0.95 show a satisfactory match between the experimental data and the D-R isotherm model, implying that the model is acceptable for explaining the adsorption process (Hasani *et al.*, 2022). In this case, both the arsenic and chromium metal ions exhibited  $R^2$  values greater than 0.95, indicating that the D-R isotherm model provided a good fit to the experimental data. This suggests that the D-R isotherm model accurately describes the adsorption process of arsenic and chromium metal ions on the neem leaf biochar at the specified temperature of 30°C. Furthermore, the  $R^2$  values computed from the Langmuir, Freundlich, and Temkin isotherm plots were compared to determine which isotherm plot provided the greatest match for the isotherm research. The findings demonstrated that the Freundlich isotherm offered the greatest match for both arsenic and chromium, followed by the Langmuir, Temkin, and D-R isotherms.

High  $R^2$  values for the Freundlich isotherm point to a multilayer adsorption mechanism occurring on the surface

**Table 2.** Isotherm constants for metal ion adsorption

Type of study	Parameters	Units	As (II)	Cr (VI)
Langmuir	$q_{\max}$	mg/g	11.293	9.348
	$K_L$	1/mol	0.419	0.501
	$R^2$	-	0.9704	0.9505
Freundlich	$K_f$	L/g	3.192	2.947
	$n$	-	3.029	2.847
	$R^2$	-	0.9557	0.9656
Temkin	$K_T$	L/Mol	$1.27 \times 10^7$	$1.88 \times 10^4$
	$b \times 10^{-6}$	J g mol <sup>-2</sup>	25.6	23.8
	$R^2$	-	0.9897	0.9502
D-R	$X_m \times 10^{-3}$	(mol/g)	4.15	3.76
	$\epsilon$	KJ/mol	11.75	10.31
	$R^2$	-	0.9983	0.9895

### 5.5. Kinetic studies

The kinetic studies were conducted at different time intervals to determine the dominant mechanism of As(II) and Cr(VI) adsorption using the neem leaf biochar material, whether it involves physical or chemical forces. By comparing the results from these kinetic studies, it will be possible to determine the dominant mechanisms of As(II) and Cr(VI) adsorption using the neem leaf biochar material and shed light on the nature of the adsorption process, whether it is primarily driven by physical interactions or chemical bonding between the metal ions and the biochar surface.

of neem leaves. On the other hand, the  $R^2$  values for the Temkin and D-R isotherms indicated a multilayer adsorption process with heterogeneous adsorption. Overall, the Freundlich isotherm study provided the greatest fit for the arsenic and chromium removal on neem leaf biochar, indicating its effectiveness in multilayer adsorption. However, the agreement of  $R^2$  values with the Temkin and D-R isotherms also suggests that these models can adequately describe the adsorption process with a multilayer and heterogeneous adsorption characteristic.

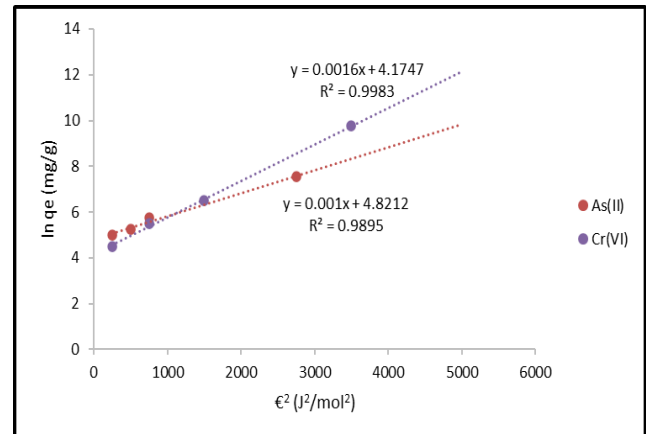


**Figure 13.** Neem leaf biochar's D-R isotherm plot for the adsorption of heavy metals

### 5.6. Pseudo first order kinetics

The linear plots  $[(q_e - q) \text{ vs. } t]$  derived from the pseudo-first-order or Lagergren model are shown in Figure 14. The linear graphs of the equation revealed the first-order rate constant ( $k$ ) and  $R^2$  values when the metal ion concentration was changed from 20 to 100 mg/L. The constants obtained from this model were presented in Table 3, with  $R^2$  values exceeding 0.95. The Lagergren model is appropriate and applicable for modelling the adsorption process, as indicated by the strong  $R^2$  values. The effectiveness of the model in fitting the experimental data suggests that the adsorption process may have reached a saturation point (Jinzheng *et al.*, 2022).

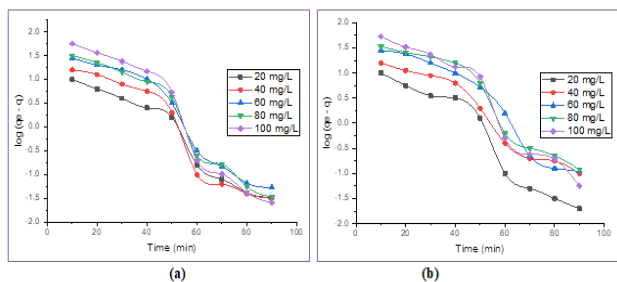


**Figure 14.** Pseudo first order plots for the adsorption of (a) As & (b) Cr heavy metal ions using neem leaf biosorbent

### 5.7. Pseudo second order kinetics

Similarly, in the second-order kinetic studies, the initial ion concentrations were adjusted to 20, 40, 60, 80, and 100 mg/L, and the corresponding constants were obtained from the linear plots as shown in Figure 15. The constants of the second-order kinetics were represented in Table 3, and they were calculated based on the linear equations derived from this study. Notably, the  $q_e$  values derived from the linear equations closely matched the  $q_e$  values obtained through experimental analysis. The second-order kinetic studies also exhibited a good fit with the adsorption process, as indicated by the plot values. This suggests that the adsorption process reached a saturation point with limiting behavior (Li *et al*, 2012). Overall, the second-order kinetic model provided further insights into the adsorption behavior of CV and MB dyes using the coconut shell biochar material, confirming the efficiency of the adsorbent in removing these dyes from aqueous solutions.

### 5.8. Boyd kinetics

Despite not passing through the origin point, the lines in the Boyd kinetic plots (Figure 16) for the adsorption of arsenic and chromium ions by neem leaf biochar were shown to be linear. This departure from the genesis point shows that external film diffusion took place while the

adsorbent was absorbing metal ions (Mustapha *et al*, 2019). By analyzing the Boyd kinetic plots, the Boyd kinetic parameters ( $D_i$  and  $B$ ) were calculated and presented in Table 3. The obtained regression values ( $R^2 > 0.95$ ) indicate a very good fit with the experimental data, further confirming the applicability of the Boyd kinetic model to describe the adsorption process of arsenic and chromium ions by neem leaf biochar.

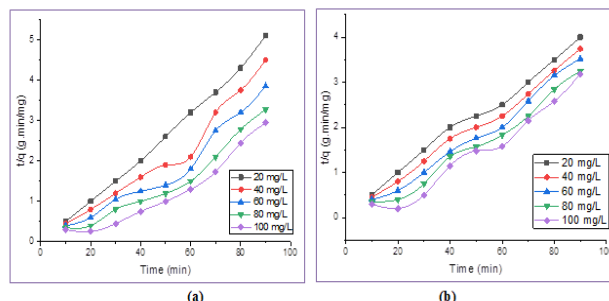


**Figure 15.** Pseudo second order plots for the adsorption of (a) As & (b) Cr heavy metal ions using neem leaf biosorbent

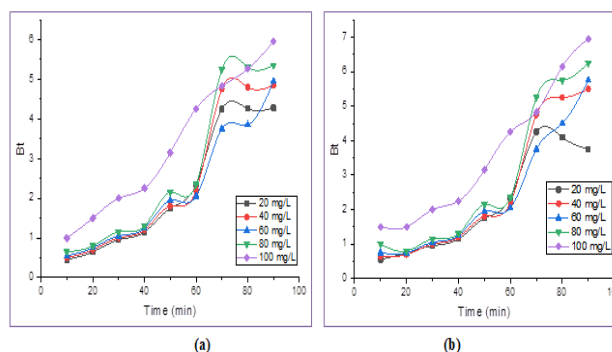


**Figure 16.** Boyd kinetic plots for the adsorption of (a) As & (b) Cr heavy metal ions using neem leaf biosorbent

**Table 3.** Adsorption kinetic constants for heavy metal removal using neem leaf biosorbent

S. No	Name of the metal ion	Conc.(mg/L)	Pseudo First order			Pseudo Second order			Boyd			
			K (min <sup>-1</sup> )	q <sub>e,cal</sub> (mg/g)	R <sup>2</sup>	K (g/mg.min) × 10 <sup>-3</sup>	q <sub>e,cal</sub> (mg/g)	h (mg/g.min)	R <sup>2</sup>	B	D <sub>i</sub> (× 10 <sup>-3</sup> m <sup>2</sup> /s)	R <sup>2</sup>
1.	As (II)	20	0.034	2.64	0.95	16.69	2.15	0.10	0.96	0.034	5.472	0.915
2.		40	0.043	7.02	0.93	5.73	5.19	0.18	0.98	0.044	7.340	0.973
3.		60	0.041	10.00	0.93	3.34	8.30	0.22	0.98	0.043	7.621	0.963
4.		80	0.039	11.36	0.94	5.07	10.75	0.26	0.98	0.039	6.856	0.914
5.		100	0.048	17.47	0.92	2.00	12.91	0.29	0.97	0.049	8.725	0.982
6.	Cr (VI)	20	0.046	3.68	0.91	12.62	2.70	0.10	0.97	0.046	7.678	0.943
7.		40	0.041	6.54	0.93	5.32	5.47	0.12	0.98	0.041	6.294	0.983
8.		60	0.043	9.95	0.92	3.56	8.60	0.23	0.98	0.045	7.959	0.924
9.		80	0.046	12.38	0.94	2.77	10.10	0.28	0.97	0.046	7.678	0.983
10.		100	0.052	20.55	0.92	2.30	11.56	0.31	0.98	0.053	8.590	0.941

### 5.9. Thermodynamic studies

The thermodynamic parameters of the adsorption process were examined by graphing the natural logarithm of the equilibrium constant ( $\log K_c$ ) against the inverse of temperature ( $1/T$ ) for various concentrations of the targeted metal ions, as shown in Figure 17 (a) & (b). The

determination of these thermodynamic properties provides valuable insights into the spontaneity and energetics of the adsorption reaction using neem leaf powder as the adsorbent. Negative  $\Delta G_0$  values indicate that the adsorption of metal ions onto the neem leaf powder is spontaneous, meaning the process tends to

occur naturally without the need for external energy input. On the other hand, positive  $\Delta H_o$  values suggest that the adsorption reaction is endothermic, requiring the input of heat for the adsorption process to proceed. This indicates that the adsorption of metal ions is favored at higher temperatures, as the system absorbs heat from the surroundings to facilitate the adsorption. Furthermore, the presence of positive  $\Delta S_o$  values during the binding of metallic ions to neem leaf powder in an aqueous media indicates an increase in system disorder or randomness when the metallic ions are adsorbed onto the adsorbent's surface. This implies that the adsorption process increases the system's entropy, which is a favorable property for boosting metal ion adsorption (Guo *et al.*, 2022). Overall, the thermodynamic study offers significant information about the adsorption process and validates neem leaf powder's applicability as an efficient adsorbent for removing specific metal ions from aqueous solutions. The thermodynamic study reveals that metal ion adsorption using neem leaf biosorbent is thermodynamically advantageous. The positive  $\Delta S_o$  values indicate an increase in entropy, suggesting that the process leads to more disorder in the system, making the adsorption energetically favorable. Additionally, the positive  $\Delta G_o$  values further support the impulsive nature of the metal ion adsorption, indicating that the process occurs naturally without the need for external energy input.

Positive  $\Delta H_o$  values, which denote the exothermic character of the adsorption process, imply that heat is given off when metal ions bind to the neem leaf

**Table 4.** Heavy metal adsorption using neem leaf powder: Thermodynamic Constants

As (II) – Initial Concentration	$\Delta H^o$ (KJ/mol)	$\Delta S^o$ (J/mol/	$\Delta G_o$ (kJ/mol)			
			15°C	30°C	45°C	60°C
20	-83.38	222.52	-15.90	-10.82	-9.24	-8.24
40	-42.73	96.87	-11.31	-8.98	-7.45	-7.32
60	-26.45	61.28	-8.60	-7.45	-6.58	-6.15
80	-19.64	41.29	-6.69	-6.72	-6.19	-5.93
100	-16.82	32.35	-6.24	-6.12	-5.68	-5.28
Cr (VI) – Initial Concentration						
20	-56.24	143.77	-13.30	-11.15	-8.93	-8.13
40	-31.69	72.86	-9.02	-8.80	-7.47	-6.69
60	-26.44	56.98	-8.12	-6.90	-6.64	-5.51
80	-19.89	39.31	-7.62	-6.09	-5.38	-5.20
100	-15.49	21.83	-6.63	-5.44	-4.92	-4.69

#### 5.10. Desorption experimental analysis

Disposal of spent adsorbent presents a significant challenge in the adsorption process and can lead to severe environmental pollution. To address this issue and make the adsorption process more economical, the regeneration of spent adsorbent is crucial. In desorption studies, metal ion recovery was achieved using concentrated hydrochloric acid with varying concentrations (ranging from 0.1N to 0.4N). During the initial stages of desorption, the recovery of heavy metal ions from the consumed adsorbent was quick. The retrieval of metal ions, however, abruptly decreased after the hydrochloric acid concentration above 0.3N and eventually stabilized. This showed that the maximum

biosorbent. This release of heat contributes to the overall energy balance of the process and indicates that the adsorption is favored at higher temperatures (Syafiuddin *et al.*, 2018). Overall, the thermodynamic parameters provide crucial information about the energy changes and feasibility of the metal ion adsorption. The thermodynamic plots and intended standards support the conclusion that the adsorption of metal ions using neem leaf biosorbent is a spontaneous, exothermic process driven by an increase in entropy (Table 4). This understanding is valuable in optimizing and designing efficient adsorption processes for water treatment and pollution remediation applications.

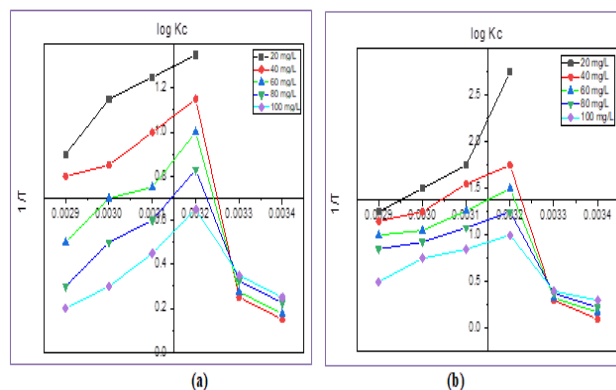


**Figure 17.** Thermodynamic plots of (a) As & (b) Cr metal ion adsorption using neem leaf powder

amount of metal ions recovery was attained with 0.3N of hydrochloric acid and that there was no further increase in desorption with a higher concentration. Using 0.3N of hydrochloric acid, the study successfully recovered approximately 87.31% of arsenic and 81.28% of chromium ions from the neem leaf biochar's surface. The possibility of metal ion recovery by desorption using hydrochloric acid and its potential for further applications were shown by the use of the recovered metal ions in several experimental operations.

## 6. Conclusion

The neem leaf biosorbent's efficacy in removing arsenic and chromium metal ions from wastewater was examined

through batch mode adsorption studies. All experimental analyses were conducted at room temperature (25°C), and the Langmuir, Freundlich, Temkin, and D-R isothermal studies confirmed a multilayer adsorption process with a heterogeneous nature. Furthermore, the pseudo-First and Second-order as well as Boyd kinetic studies verified that the uptake of metal ions by the neem leaf adsorbent followed a chemical adsorption process. Thermodynamic studies revealed the exothermic nature of metal ion adsorption. In desorption studies, 89.74% of arsenic ions and 82.32% of chromium ions were successfully recovered by adding concentrated hydrochloric acid. These findings demonstrate the potential of neem leaf biosorbent as an effective means of removing heavy metal ions from wastewater and highlight its capacity for desorption and metal ion recovery.

## References

- Adeyemo A.A., Adeoye I.O. and Bello O.S. (2015). Adsorption of dyes using different types of clay: a review, *Applied Water Science*, **7**, 543–568. <https://doi.org/10.1007/s13201-015-0322-y>
- Agarwal S., Tyagi I., Gupta V.K., Dehghani M.H., Jaafari J., Balarak D. and Asiff M. (2016). Rapid removal of noxious nickel (II) using novel  $\gamma$ -alumina nanoparticles and multiwalled carbon nanotubes: Kinetic and isotherm studies, *Journal of Molecular Liquids*, **224**, 618–623. <https://doi.org/10.1016/j.molliq.2016.10.032>
- Aydina S., Nura H.M., Traorea A.M., Yildirimb E. and Emik S. (2021). Fixed bed column adsorption of vanadium from water using amino-functional polymeric adsorbent, *Desalination and Water Treatment*, **209**, 280–288. <https://doi.org/10.5004/dwt.2021.26493>
- Batagarawa S.M. and Ajibola A.K. (2019). Comparative evaluation for the adsorption of toxic heavy metals on to millet, corn and rice husks as adsorbents. *Journal of Analytical and Pharmaceutical Research*, **3**, 119–125. Doi: <https://doi.org/10.15406/japlr.2019.08.00325>
- Benjelloun M., Miyah Y., Evrendilek G.A. and Lairini F.Z.S. (2021). Recent Advances in Adsorption Kinetic Models: Their Application to Dye Types, *Arabian Journal of Chemistry*, **14** (4), 103031. <https://doi.org/10.1016/j.arabjc.2021.103031>
- Bouras H.D., Benturki O., Bouras N., Attou M., Donnot A., Merlin A., Addoun F. and Holtz M.D. (2015). The use of an agricultural waste material from *Ziziphus jujuba* as a novel adsorbent for humic acid removal from aqueous solutions. *Journal of Molecular Liquids*, **211**, 1039–1046. Doi: <https://doi.org/10.1016/j.molliq.2015.08.028>
- Condurache B.C., Cojocaru C., Samoila P., Cosmulescu S.F., Predeanu G., Enache A.C. and Harabagiu V. (2022). Oxidized Biomass and Its Usage as Adsorbent for Removal of Heavy Metal Ions from Aqueous Solutions. *Molecules*, **27**, 6119. <https://doi.org/10.3390/molecules27186119>
- Dulla J.B., Tamana M.R., Boddu S., Pulipati K. and Srirama K. (2020). Biosorption of copper (II) onto spent biomass of *Gelidiella acerosa* (brown marine algae): optimization and kinetic studies, *Applied Water Science*, **10** (56). <https://doi.org/10.1007/s13201-019-1125-3>
- Fideles R.A., Teodoro F.S., Xavier A.L., Adarme O.F.H., Gil L.F. and Gurgel L.V.A. (2019). Trimellitated sugarcane bagasse: A versatile adsorbent for removal of cationic dyes from aqueous solution. Part II: Batch and continuous adsorption in a bicomponent system, *Journal of Colloid and Interface Science*, **552** (15), 752–763. <https://doi.org/10.1016/j.jcis.2019.05.089>
- Guo X., Liu A., Lu J., Niu X., Jiang M., Ma Y., Liu X. and Li M. (2020). Adsorption Mechanism of Hexavalent Chromium on Biochar: Kinetic, Thermodynamic, and Characterization Studies, *ACS Omega*, **5** (42), 27323–27331. DOI: 10.1021/acsomega.0c03652
- Haro N.K., Dávila I.V.J., Nunes K.G.P., de Franco M.A.E., Marcilio N.R. and Féris L.A. (2021). Kinetic, equilibrium and thermodynamic studies of the adsorption of paracetamol in activated carbon in batch model and fixed-bed column, **11** (38). <https://doi.org/10.1007/s13201-020-01346-5>
- Hasani N., Selimi T., Mele A., Thaçi V., Halili J., Berisha A. and Sadiku M. (2022). Theoretical, Equilibrium, Kinetics and Thermodynamic Investigations of Methylene Blue Adsorption onto Lignite Coal. *Molecules*, **27**, 1856. <https://doi.org/10.3390/molecules27061856>
- Hong J., Xie J., Mirshahghassemi S. and Lead J. (2020). Metal (Cu, Cr, Ni, Pb) removal from environmentally relevant waters using polyvinylpyrrolidone – coated magnetic nanoparticles. *RSC advances*, **10**, 3266–3276. Doi: <https://doi.org/10.1039/C9RA10104G>
- Hosseinzehi M., Khatebasreh M. and Dalvand A. (2020). Modeling of Reactive Black 5 azo dye adsorption from aqueous solution on activated carbon prepared from poplar sawdust using response surface methodology, *International Journal of Environmental Analytical Chemistry*, **18**. <https://doi.org/10.1080/03067319.2020.1819991>
- Ji L., Xie S., Feng J., Li Y. and Chen L. (2012). Heavy metal uptake capacities by the common freshwater green alga *Cladophora fracta*, *Journal of Applied Psychology*, **24**, 979–983. <https://doi.org/10.1007/s10811-011-9721-0>
- Kołodęńska D., Bąk J. and Thomas P. (2016). Comparison of Sorption and Desorption Studies of Heavy Metal Ions from Biochar and Commercial Active Carbon. *Chemical Engineering Journal*, **307**. Doi: <http://dx.doi.org/10.1016/j.cej.2016.08.088>
- Konicki W., Aleksandrak M., Moszyński D. and Mijowska E. (2017). Adsorption of anionic azo-dyes from aqueous solutions onto graphene oxide: Equilibrium, kinetic and thermodynamic studies, *Journal of Colloid and Interface Science*, **496**, 188–200. <https://doi.org/10.1016/j.jcis.2017.02.031>
- Labied R., Benturki O., Hamitouche A.Y.E. and Donnot A. (2018). Adsorption of hexavalent chromium by activated carbon obtained from a waste lignocellulosic material (*Ziziphus jujuba* cores): Kinetic, equilibrium, and thermodynamic study. *Adsorption Science and Technology*, **36** (3–4), 1066–1099. Doi:10.1177/0263617417750739
- Ma J., Hou L., Li P., Zhang S. and Zheng X. (2022). Modified fruit pericarp as an effective biosorbent for removing azo dye from aqueous solution: study of adsorption properties and mechanisms, *Environmental Engineering Research*, **27** (2), 200634. <https://doi.org/10.4491/eer.2020.634>
- Malti W.E., Hijazi A., Khalil Z.A., Yaghi Z., Medlej M.K. and Reda M. (2022). Comparative study of the elimination of copper, cadmium, and methylene blue from water by adsorption on



- the citrus Sinensis peel and its activated carbon, *RSC Advances*, **12**, 10186. <https://doi.org/10.1039/D1RA08997H>
- Manjuladevi M., Anitha R. and Manonmani S. (2018). Kinetic study on adsorption of Cr (VI), Ni (II), Cd (II) and Pb (II) ions from aqueous solutions using activated carbon prepared from cucumis melo peel. *Applied water science*, **8** (36). <https://doi.org/10.1007/s13201-018-0674-1>
- Mustapha S., Shuaib D.T., Ndamitso M.M. *et al.* (2019). Adsorption isotherm, kinetic and thermodynamic studies for the removal of Pb(II), Cd(II), Zn(II) and Cu(II) ions from aqueous solutions using *Albizia lebbek* pods. *Applied Water Science* **9**, 142. <https://doi.org/10.1007/s13201-019-1021-x>
- Omer M., Khan B., Khan I., Alamzeb M., Zada F.M., Ullah I., Shah R., Alqarni M. and Simal-Gandara J. (2022). Kinetic and Thermodynamic Studies for the Adsorption of Metanil Yellow Using Carbonized Pistachio Shell-Magnetic Nanoparticles. *Water*, **14**, 4139. <https://doi.org/10.3390/w14244139>
- Phuengphai P., Singjanusong T., Kheangkhun N. and Wattanakornsiri A. (2021). Removal of copper (II) from aqueous solution using chemically modified fruit peels as efficient low-cost biosorbents, *Water Science and Engineering*, **14** (4), 286–294. <http://dx.doi.org/10.1016/j.wse.2021.08.003>
- Priya A.K., Yogeshwaran V., Rajendran S., Tuan K.A. Hoang, Matias Soto-Moscoco, Ayman A. Ghfar and Chinna Bathula (2022). Investigation of mechanism of heavy metals ( $\text{Cr}^{6+}$ ,  $\text{Pb}_{2+}$  &  $\text{Zn}^{2+}$ ) adsorption from aqueous medium using rice husk ash: Kinetic and thermodynamic approach, *Chemosphere*, **286**, 131796. <https://doi.org/10.1016/j.chemosphere.2021.131796>
- Regti A., Laamari M.R., Stiriba S.E. and El Haddad M. (2017). The potential use of activated carbon prepared from Ziziphus species for removing dyes from waste waters. *Applied Water Science*, **7**, 4099–4108. Doi: <https://doi.org/10.1007/s13201-017-0567-8>
- Revellame E.D., Fortela D.L., Sharp W., Hernandez R. and Zappi M.E. (2020). Adsorption kinetic modeling using pseudo-first order and pseudo-second order rate laws: A review, *Cleaner Engineering and Technology*, **1**, 100032. <https://doi.org/10.1016/j.clet.2020.100032>
- Singh J., Dhiman N. and Sharma N.K. (2018). Effect of Fe(II) on the Adsorption of Mn(II) from Aqueous Solution Using Esterified Saw Dust: Equilibrium and Thermodynamic Studies. *Indian Chemical Engineer*, **60** (3), 255–268. <https://doi.org/10.1080/00194506.2017.1363674>
- Sirusbakht S., Vafajoo L., Soltani S. and Habibi S. (2018). Sawdust Bio sorption of Chromium (VI) Ions from Aqueous Solutions. *Chemical Engineering Transactions*, **70**, 1147–1152. <https://doi.org/10.3303/CET1870192>
- Stefanik J., Dutta A., Verbinnen B., Shakya M. and Rane E.R. (2018). Selenium removal from mining and process wastewater. A systematic review of available technologies, *67* (8), 903–918. <https://doi.org/10.2166/aqua.2018.109>
- Syafiuddin A., Salmiati S., Jonbi J. and Fulazzaky M.A. (2018). Application of the kinetic and isotherm models for better understanding of the behaviors of silver nanoparticles adsorption onto different adsorbents, *Journal of Environmental Management*, **15**, 59–70. <https://doi.org/10.1016/j.jenvman.2018.03.066>
- Venkatraman Y. and Priya A.K. (2021). Removal of heavy metal ion concentrations from the wastewater using tobacco leaves coated with iron oxide nanoparticles, *International Journal of Environmental Science and Technology*, **19**, 2721–2736. <https://doi.org/10.1007/s13762-021-03202-8>
- Wang C., Wang X., Li N., Tao J.2., Yan B., Cui X. and Chen G. (2022). Adsorption of Lead from Aqueous Solution by Biochar: A Review. *Clean Technologies*, **4**, 629–652. <https://doi.org/10.3390/cleantechnol4030039>
- Xi L., Zhou S., Zhang C., Fu Z., Wang A., Zhang Q., Wang Y., Liu X., Wang X. and Xua W. (2020). Environment-friendly Juncus effusus-based adsorbent with a three-dimensional network structure for highly efficient removal of dyes from wastewater, *Journal of Cleaner Production*, **259**, 120812. <https://doi.org/10.1016/j.jclepro.2020.120812>